Materials Research Proceedings 40 (2024) 294-302 https://doi.org/10.21741/9781644903117-31

Structural Characterization of Stone Flooring "Calçada Marble", in Lisbon, Portugal

Mohamed EL OMARI[1,a], Mohamed EL AMRAOUI[1,b *], Imane FIKRI[1,c], Lahcen BEJJIT[1,d], Mustapha HADDAD[1,e], Saadia AIT LYAZDI[1,f], Aumeur EL AMRANI[1,g]

[1]Laboratory of Spectrometry, Materials and Archaeomaterials (LASMAR), URL CNRST N° 7 Faculty of Sciences, Moulay Ismail University of Meknes, P.O Box 11201 Zitoune, Meknes, Morocco

[a]moh4med.elomari@gmail.com, [b]m.elamraoui@umi.ac.ma, [c]imane.fikri16@gmail.com, [d]l.bejjit@umi.ac.ma, [e]mhaddad22@yahoo.fr, [f]aitlyazidisaadia@yahoo.fr, [g]a.elamrani@fste.umi.ac.ma

Keywords: Raman Spectroscopy, ATR-FTIR, XRD, Characterization, Mineralogical Phase, Flooring, Calçada

Abstract. The Lisbon "Calçada" sidewalks have a traditional style made of small flat and irregular cobblestones, representing magnificent mosaics. This work presents the characterization and identification of the mineralogical phases of sidewalk stones, originating from Lisbon, Portugal. Samples referenced MEKPBL (white) and MEKPNL (grey-black) were studied by means of Raman spectroscopy, ATR-FTIR and XRD. All Raman spectra show a strong band around 1089 cm^{-1} which can be attributed to the v_1-symmetric stretching mode of $(CO3)^{2-}$, indicating that calcite is the main crystal phase in both samples. All Raman spectra of MEKPNL show also graphite fingerprints localized around 1329 cm^{-1} and 1607 cm^{-1}, which are characteristic respectively of the D and G peaks of the carbonaceous material. These carbonaceous materials are the substance responsible of the grey-black color to these stones. Furthermore, the Raman spectra of the MEKPNL sample show also a weak Raman band located at 460 cm^{-1} which can be attributed to the symmetrical stretching of Si-O-Si, characteristic of the α-quartz. Furthermore, ATR-FTIR and XRD analyses supported the Raman results.

Introduction

Since antiquity, stone's mechanical and thermal properties have allowed it to be used for many applications [1, 2], particularly in funerary art as structural elements in buildings and architectural monuments, as well as in the paving and ornamentation of sidewalks and roads [2, 3]. Therefore, in the 19th century, a traditional flooring style that is part of Portugal's cultural heritage, called "calçada portuguesa", was introduced to most of the pavements in Portugal regions. It consists of small, flat stones arranged irregularly to form patterns or images, creating a mosaic-like appearance [2-5]. These stones come from various quarries, with some found in Portuguese regions such as Estremoz, Borba, and Vila Viçosa, while others are found in different countries, such as Italy, Greece and Spain [2]. Furthermore, this style of pavement can also be found in cities worldwide, from Olivenza (under Spanish colonial era), to former Portuguese colonies like Goa in India, and even the countries influenced by Portuguese culture, such as Brazil and Mozambique [3].

The investigation of the mineralogical composition of decorative stones, even those used in paving, requires the integration of multiple analysis techniques. Their correlation can provide crucial knowledge about these materials and manufacturing techniques, as well as solve problems related to their conservation/restoration of historical monuments, sculptures and architectural structures, including floor pavements. In this context, we find that Raman spectroscopy, ATR-

FTIR (Attenuated total reflectance-Fourier transform infrared) spectroscopy and XRD (Powder X-ray diffraction) analysis, are widely used techniques to identify the crystalline phases of ornamental stones [6, 7]. Additionally, Raman spectroscopy has been applied as a tool for examining the phases of different types of carbonaceous matter present in rocks and stones, such as kerogen, amorphous carbon, carbon, solid bitumens as well as graphite [8].

Hence, the work here aims to characterize and identify the mineralogical composition of two decorative stones coming from Lisbon; they are used to ornament the pavements of Calçada. The analysis was carried out using a combination of structural techniques including Raman spectroscopy, ATR-FTIR spectroscopy and XRD.

Materials and Methods

Materials

Two natural stones of almost identical size, originating from Lisbon, Portugal; they are the subject of a study using a multi-technique approach. These samples stones are referenced in LASMAR laboratory as MEKPNL and MEKPBL. The color of MEKPBL is white, while MEKPNL varies from grey to black. The stone samples were manually crushed using an agate mortar and pestle. The obtained powders were used for Raman and XRD analysis. For ATR-FTIR analysis, the powders were sieved to a grain size of ≤ 50 µm. Photos and a brief description of the stones studied are given in Table 1.

Table 1: Samples codes, photos, color and their origin.

Sample	Photo	Color	Origin
MEKPBL		White	Lisbon, Portugal
MEKPNL		Gray-black	Lisbon, Portugal

This type of stones has many heritage uses, particularly for paving the Portuguese Calçada. Fig.1 shows a particular section of the Lisbon pavement, made from small flat stones (white and black) arranged in traditional mosaic patterns.

Materials Research Proceedings 40 (2024) 294-302 https://doi.org/10.21741/9781644903117-31

Fig. 1: Center of Lisbon and particular sections of Calçada pavement in Lisbon.

Characterization methods

Micro-Raman spectroscopy

Raman spectra were carried out using the Renishaw RM 1000 confocal spectrometer. It's equipped with an (He-Ne) laser excitation source operating at 632.8 nm, an electrically cooled CCD detector and a DMLM confocal microscope with different objectives (10x, 20x, 50x and 100x). The spectra were recorded in the wavenumber range of 100 - 2000 cm^{-1} with a resolution less than of 2 cm^{-1}. Calibration was performed using the 520 cm^{-1} Raman line of a silicon wafer. Repeated acquisition using the highest magnification was accumulated to improve the signal to noise ratio. The Laser power was set between 10 and 50 mW in order to avoid degradation and decomposition of sample. Data were collected and plotted using the WIRE 3.4 software.

ATR-FTIR spectroscopy

Infrared spectra were obtained from powdered samples using an Alpha-Bruker spectrometer equipped with an ATR accessory equipped with a diamond crystal. The spectra were recorded in the wavenumber range from 400 to 4000 $cm^{-}1$ with a spectral resolution of 4 $cm^{-}1$.

X-ray Diffraction (XRD)

The stone samples were characterized in powder form through X-ray diffraction at room temperature. This analysis was carried out using an ADVANCE D8 X-ray diffractometer, available at the Innovation and Technology Transfer Centre (CITT) of Moulay Ismaïl University, Morocco. It's equipped with Cu-Kβ radiation (wavelength of 1.5418 Å with 40 mA and 45 kV). The diffraction patterns were performed in the 2θ range of 5° - 80° with a step of 2° per minute. In addition, the various Bragg reflections are indexed using the RUFF database and the ICDD PDF-4 files [9, 10].

Results and discussion

Micro-Raman analyses

Fig. 2 presents the Raman spectra of the MEKPBL and MEKPNL samples, recorded in 150-2000 cm^{-1} range. It's evident from the spectra that both stones exhibit characteristic bands around 160, 286, 717 and 1089 cm^{-1}. The stronger band at 1089 cm^{-1} is attributed to the ν_1-symmetric stretching mode of CO_3^{2-} ionic group. The band at 717 cm^{-1} is assigned to the ν_4- symmetric

bending mode of CO_3^{2-}. The two bands at 160 and 286 cm-1 are related to the external vibrations, the relative translation between the CO_3^{2-} group and the Ca^{2+} cation (Ca^{2+}, CO_3^{2-})). These bands are the characteristics of the calcite ($CaCO_3$), which means that both samples can be classified as limestones composed mainly of calcite ($CaCO_3$) [1, 11-13].

The typical Raman bands of calcite ($CaCO_3$) observed in the studied limestones are consistent with those reported by S. Gunasekaran et al. (2006) of a natural limestone sourced from India, which is characterized at room temperature through FT-Raman spectroscopy, FTIR spectroscopy and XRD [12]. According to their Raman results, the external vibration modes (T (Ca^{2+}, CO_3^{2-})) were observed at 162 and 288 cm^{-1}. The symmetric bending mode (ν_2 (CO_3^{2-})) at 716 cm^{-1}, while the symmetric stretching mode ν_1 (CO_3^{2-}) at 1092 cm^{-1}.

An additional wide band is observed in both stones at 460 cm^{-1}, which can be assigned to the symmetrical stretching mode of Si-O-Si; it's the characteristic of α-quartz (SiO_2) [14- 16].

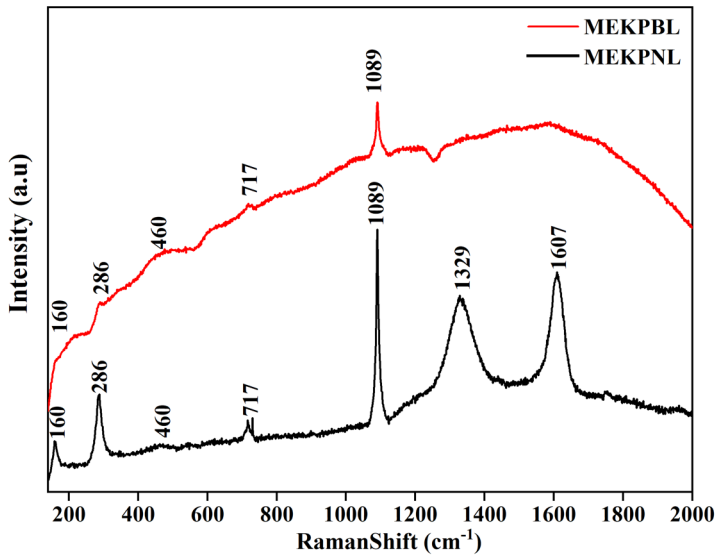

Fig. 2: Raman spectra of MEKPNL and MEKPBL samples.

The Raman spectrum of MEKPNL stone exhibits also two supplementary bands located around 1329 cm^{-1} and 1607 cm^{-1}; which are the fingerprints of the graphite (C) [1, 8, 17]. The first one at 1329 cm^{-1} is attributed to the D band, linked to disordered carbon or defective graphitic structures. Whereas those at 1607 cm^{-1} can be assigned to G band, the first-order Raman band of graphitic matter [8, 17, 21]. We can notice that graphite is the responsible element for the gray-black color of MEKPNL [1, 8, 17].

The Raman signals corresponding to graphite(C), detected in the MEKPNL spectrum are similar to those reported in the works of Raneri S. et al. (2020) [17]. The mentioned study focused on the characterization of three decorative black limestones from Tolfa region in Italy using Raman spectrometry. Consequently, the Raman band positions of these three black limestones were observed as follows: 1345, 1339 and 1334 cm^{-1} for the D bands and 1607, 1607 and 1609 cm^{-1} for the G bands, respectively.

ATR-FTIR analyses

ATR-FTIR spectra recorded in the 400-4000 cm^{-1} range of the MEKPBL and MEKPNL stones are illustrated in Fig. 3; they showed absorption bands at 711, 872, 1401 and 1794 cm^{-1}. The two strongest bands at 1401 cm^{-1} and 872 cm^{-1} are attributed to the asymmetric stretching (ν_3) and bending (ν_2) modes of the CO_3^{2-} ionic group, respectively. The band at 711 cm^{-1} is attributed to

the ν_4-asymmetric bending of the CO_3^{2-} group. The weak line at 1794 cm^{-1} is assigned to the combined modes ($\nu_1 + \nu_4$) [12, 13]. These bands are characteristic of calcite ($CaCO_3$).

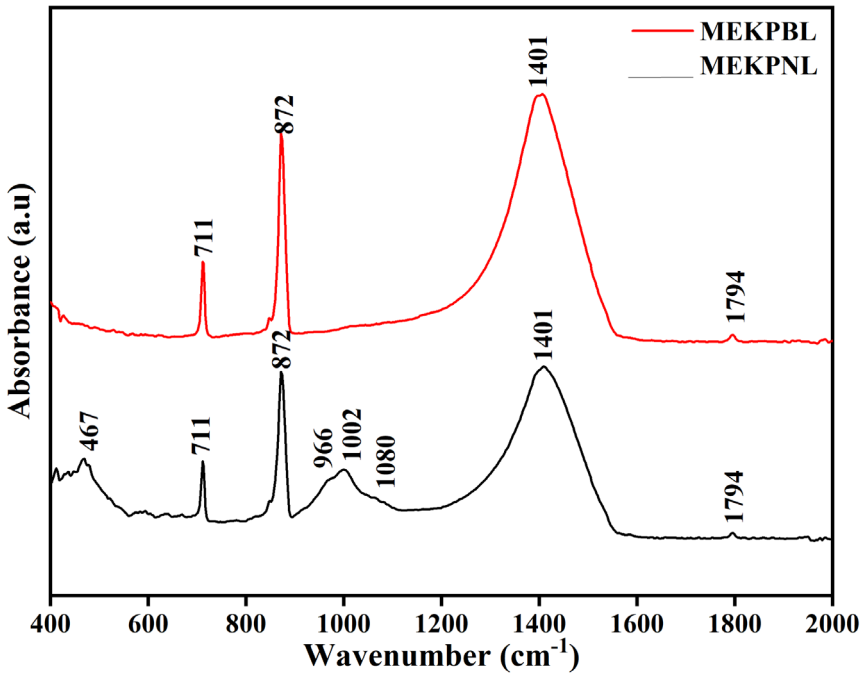

Fig. 3: ATR-FTIR spectra of MEKPNL and MEKPBL samples.

In addition, the spectrum of MEKPNL displays bands located at 467, 966, 1002 cm^{-1} and 1080 cm^{-1}, characteristic of the α-quartz (SiO_2) [14, 18, 19]. The band at 467 cm^{-1} is attributed to the asymmetric bending vibrations mode of Si-O-Si groups [18-20]. The both bands that are appear at 1002 and 1080 cm^{-1} are assigned to the asymmetric stretching mode of Si-O groups [18, 20], while the band at 966 cm^{-1} is attributed to the bending vibration of Si-O-(H-H_2O) [20].

The assignment of Raman and infrared bands for the two stones studied are given in Table 2, besides the identification of the mineralogical phases achieved through Raman and ATR-FTIR spectroscopy.

Materials Research Proceedings 40 (2024) 294-302 https://doi.org/10.21741/9781644903117-31

Table 2: Bands assignment and mineralogical compositions of Raman and ATR-FTIR analyses of MEKPBL and MEKPNL stones.

Sample	Band positions (cm^{-1})		Assignment	Mineralogical composition
	Raman	Infrared		
MEKPBL	160-286	—	T (Ca^{2+}, CO_3^{2-})	Calcite ($CaCO_3$)
	717	711	ν_4-(CO_3^{2-})	
	—	872	ν_2-(CO_3^{2-})	
	1089	—	ν_1 (CO_3^{2-})	
	—	1401	ν_3 (CO_3^{2-})	
	—	1794	ν_{1+} ν_4	
	460	—	Symmetric stretching of Si-O-Si	α- quartz (SiO_2)
MEKPNL	160-286	—	T (Ca^{2+}, CO_3^{2-})	Calcite ($CaCO_3$)
	717	711	ν_4-(CO_3^{2-})	
	—	872	ν_2-(CO_3^{2-})	
	1089	—	ν_1 (CO_3^{2-})	
	—	1401	ν_3 (CO_3^{2-})	
	—	1794	ν_{1+} ν_4	
	460	—	Symmetric stretching of Si-O-Si	α- quartz (SiO_2)
	—	467	Asymmetric bending of Si-O-Si	
	—	966	bending of Si-O-(H-H_2O)	
	—	1002-1080	Asymmetric stretching of Si-O-Si	
	1329	—	D band	Graphite (C)
	1607	—	G band	

X-ray diffraction analyses

Fig. 4 presents the X-ray Diffraction patterns of the studied stones. As shown, both MEKPNL and MEKPBL samples exhibit a predominant line located at 2θ = 29.4°, attributed to calcite ($CaCO_3$), along with other peaks clearly observed and related to same component. MEKPBL and MEKPNL are calcitic stones. In addition, a weak line is observed in the MEKPBL sample at 2θ = 26.65°, that may correspond to α-quartz (SiO_2). The diffraction lines attributed to calcite and quartz are in good agreement with those reported in other works [1, 12, 21].

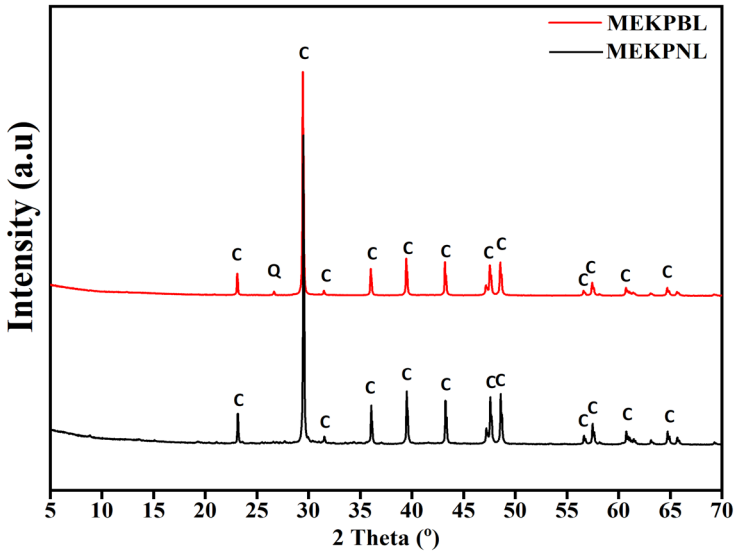

Fig. 4: XRD patterns of MEKPBL and MEKPNL samples. [C-calcite, Q- α-quartz]

The identification of the mineralogical compositions of the two studied stones MEKPBL and MEKPNL, through Raman spectroscopy, ATR-FTIR spectroscopy and XRD analysis are combined and summarized in Table 3.

Table 3: Mineralogical compositions of MEKPBL and MEKPNL stones.

Sample code	Origin	Main Phase	Other Phases
MEKPNL	Lisbon, Portugal	Calcite ($CaCO_3$)	α-quartz (SiO_2), Graphite (C)
MEKPBL	Lisbon, Portugal	Calcite ($CaCO_3$)	α-quartz (SiO_2)

The predominance of calcite ($CaCO_3$) indicates that the stones are limestone-based, which can have important implications durability and strength of the pavement [22, 23]. The presence of α-quartz (SiO_2) increases their impact resistance and strength [22, 23]. Additionally, the detection of graphite (C) through Raman spectroscopy suggests potential contributions to the mechanical properties [24, 25].

Conclusion

This study is part of an extensive study of two ornamental paving stones, originating from Lisbon, Portugal. The main objective is to determine the physical and chemical properties of these materials, where we characterize them through of multi-analytical techniques such as XRF, XRD, FORS, Raman spectroscopy, ATR-FTIR spectroscopy, EPR, and others methods can be applied.

The primary study, our focus was to characterize them in order to identify their mineralogical compositions. We used a combination of three structural spectroscopic techniques, including Raman spectroscopy, ATR-FTIR and XRD. This correlation shows that the calcite ($CaCO_3$) is the main mineralogical phase in the two identified limestones, with the presence of the α-quartz (SiO_2) in low content. Furthermore, micro-Raman spectroscopy show their ability to identify the graphitic nature of the MEKPNL stone, which is the responsible for its gray-black color.

References

[1] S. Khrissi, M. Haddad, L. Bejjit, S. A. Lyazidi, M. El Amraoui, C. Falguères, Raman and XRD characterization of Moroccan Marbles, IOP Conf. Ser: Mater. Sci. Eng. 186, (2017) 012028. https://doi.org/10.1088/1757-899X/186/1/012028

[2] J. Menningen, S. Siegesmund, L. Lopes et al. The Estremoz marbles: an updated summary on the geological, mineralogical and rock physical characteristics. Environ Earth Sci 77, (2018) 191. https://doi.org/10.1007/s12665-018-7328-3

[3] C.M. da Silva, S. Pereira. Walking on Geodiversity: the Artistic Stone-Paved Sidewalks of Lisbon (Portugal) and Their Heritage Value. Geoheritage 14, (2022) 98. https://doi.org/10.1007/s12371-022-00733-5

[4] D. Pacheco, J. Cotas, A. Domingues, S. Ressurreição, K. Bahcevandziev, L. Pereira. Chondracanthus teedei var. lusitanicus: the nutraceutical potential of an unexploited marine resource. Marine Drugs, 19(10), (2021) 570. https://doi.org/10.3390/md19100570

[5] Y. Chen, J. Fan. An applied study of Calçada Portuguesa in a former Portuguese colonial cityTake Goa, India as an example. India as an example. SSRN. (June 1, 2022). http://dx.doi.org/10.2139/ssrn.4145685

[6] A. Rousaki, P. Vandenabeele. In situ Raman spectroscopy for cultural heritage studies. Journal of Raman Spectroscopy, 52(12), (2021) 2178-2189. https://doi.org/10.1002/jrs.6166

[7] A. Boukir, S. Fellak, P. Doumenq. Structural characterization of Argania spinosa Moroccan wooden artifacts during natural degradation progress using infrared spectroscopy (ATR-FTIR) and X-Ray diffraction (XRD). Heliyon, 5(9). (2019).

https://doi.org/10.1016/j.heliyon.2019.e02477

[8] J. Jehlička, A. Šťastná, R. Přikryl. Raman spectral characterization of dispersed carbonaceous matter in decorative crystalline limestones. Spectrochimica Acta Part A: Molecular and Biomolecular Spectroscopy, 73(3), (2009) 404-409. https://doi.org/10.1016/j.saa.2008.09.006

[9] https://rruff.info/ (accessed August 20, 2023)

[10] www.icdd.com/pdfsearch/ (accessed September 25, 2023).

[11] N. Buzgar, A. I. Apopei. The Raman study of certain carbonates. Geologie Tomul L, 2(2), (2009) 97-112. https://www.researchgate.net/publication/210110408

[12] S. Gunasekaran, G. Anbalagan, S. Pandi. Raman and infrared spectra of carbonates of calcite structure. Journal of Raman Spectroscopy: An International Journal for Original Work in all Aspects of Raman Spectroscopy, Including Higher Order Processes, and also Brillouin and Rayleigh Scattering, 37(9), (2006) 892-899. https://doi.org/10.1002/jrs.1518

[13] Y. Kim, M. C. Caumon, O. Barres, A. Sall, J. Cauzid. Identification and composition of carbonate minerals of the calcite structure by Raman and infrared spectroscopies using portable devices. Spectrochimica Acta Part A: Molecular and Biomolecular Spectroscopy, 261, (2021) 119980.. https://doi.org/10.1016/j.saa.2021.119980

[14] M. Ostroumov, E. Faulques, E. Lounejeva. Raman spectroscopy of natural silica in Chicxulub impactite, Mexico. Comptes Rendus Geoscience, 334(1), (2002) 21-26.. https://doi.org/10.1016/S1631-0713(02)01700-5

[15] R. Palmeri, M. L. Frezzotti, G. Godard, R. J. Davies. Pressure-induced incipient amorphization of α-quartz and transition to coesite in an eclogite from Antarctica: a first record and some consequences. Journal of Metamorphic Geology, 27(9), (2009) 685-705.. https://doi.org/10.1111/j.1525-1314.2009.00843.x

[16] S. K. Sharma, A. K. Misra, S. Ismail, U. N. Singh. Remote Raman spectroscopy of various MIXED and composite mineral phases at 7.2 m distance. 37th Lunar and Planetary Science Conference, (2006). https://ntrs.nasa.gov/20060010179

[17] S. Raneri, F. Košek, L. Lazzarini, D. Wielgosz-Rondolino, J. Jehlicka, F. Antonelli. Raman spectroscopy as a tool for provenancing black limestones (bigi morati) used in antiquity. Journal of Raman Spectroscopy, 52(1), (2021) 241-250. https://doi.org/10.1002/jrs.5948

[18] P. Makreski, G. Jovanovski, T. Stafilov, B. Boev. Minerals from Macedonia XII. The dependence of quartz and oral color on trace element composition-AAS, FT IR and MICRO-RAMAN spectroscopy study. Bulletin of the Chemists and Technologists of Macedonia, 23(2), (2004) 171-184. https://eprints.ugd.edu.mk/id/eprint/2449

[19] F. Bosch-Reig, J. V. Gimeno-Adelantado, F. Bosch-Mossi, A. Doménech-Carbó. Quantification of minerals from ATR-FTIR spectra with spectral interferences using the MRC method. Spectrochimica Acta Part A: Molecular and Biomolecular Spectroscopy, 181, (2017) 7-12 https://doi.org/10.1016/j.saa.2017.02.012

[20] I. Ramalla, R. K. Gupta, K. Bansal. Effect on superhydrophobic surfaces on electrical porcelain insulator, improved technique at polluted areas for longer life and reliability. Int. J. Eng. Technol, 4(4), (2015) 509. https://doi.org/10.14419/ijet.v4i4.5405

[21] O. Beyssac, B. Goffé, J. P. Petitet, E. Froigneux, M. Moreau, J. N. Rouzaud. On the characterization of disordered and heterogeneous carbonaceous materials by Raman spectroscopy. Spectrochimica Acta Part A: Molecular and Biomolecular Spectroscopy, 59(10), (2003) 2267-2276. https://doi.org/10.1016/S1386-1425(03)00070-2

[22] T. M. B. Senarathna, SHMPK. Janith, A. Dassanayake, S. P. Chaminda, C L. Jayawardena, Correlations between durability, mineralogy and strength properties of limestone (2021). https://www.researchgate.net/publication/361683014

[23] P. Q. Zhao, L. C. Lu, S. D. Wang. Influence of high-silicon limestone on mineral structure and performance of belite-barium calcium sulphoaluminate clinker. Advanced Materials Research, 168, (2011) 460-465. https://doi.org/10.4028/www.scientific.net/AMR.168-170.460

[24] V. Černý, G. Yakovlev, R. Drochytka, Š. Baránek, L. Mészárosová, J. Melichar, R. Hermann. Impact of Carbon Particle Character on the Cement-Based Composite Electrical Resistivity. Materials, 14(24), (2021) 7505. https://doi.org/10.3390/ma14247505

[25] Z. Ren, J. Sun, W. Tang, X. Zeng, H. Zeng, Y. Wang, X. Wang. Mechanical and electrical properties investigation for electrically conductive cementitious composite containing nano-graphite activated magnetite. Journal of Building Engineering, 57, (2022) 104847. https://doi.org/10.1016/j.carbon.2004.12.033